Isolated Molecular Ion Solvation at an Oil/Water Interface Investigated by Vibrational Sum-Frequency Spectroscopy

Lawrence F. Scatena and Geraldine L. Richmond*

Department of Chemistry, University of Oregon, Eugene, Oregon 97403

Received: April 13, 2004; In Final Form: June 1, 2004

The structure, orientation, and intermolecular hydrogen bonding environment of H_2O molecules solvating molecular ions of surfactants adsorbed at the organic/water interface has been examined by vibrational sum-frequency spectroscopy. Vibrational spectra in the 3000−3800 cm^{-1} region are shown to be highly sensitive to the OH stretching modes of interfacial solvating H_2O molecules. Results demonstrate that the hydrogen bonding of water molecules at the CCl_4/H_2O interface in the presence of an isolated surfactant is significantly weaker than that observed near a uniform distribution of interfacial charge (saturated monolayer). Near an isolated surfactant, solvating water molecules that reside in the aqueous and organic-rich phases produce spectral features between 3500 and 3620 cm^{-1}, an indication that these solvating water molecules have weaker H_2O-H_2O interactions than those observed in bulk water. These water molecules are preferentially oriented in response to strong charge−dipole interactions. As the surface density of charged surfactants is systematically augmented the stretching modes of solvating water molecules shift to longer wavelengths, an indication that the accumulation of surface charge induces structural changes to the solvating water.

Introduction

A complete understanding of the molecular-level interactions and structural characteristics of ion solvation at an aqueous/nonaqueous interface is essential to fully comprehend some of the most fundamental processes and architecture of living organisms. The behavior of biological membranes and macromolecules, surface-active agents, and ion transport across an interface all hinge on the interplay between water and ions in an interfacial solvation process.[1,2] These complex interactions are not well understood, thus hampering the development of accurate molecular models that help make the microscopic world tangible. Consequently, investigating the solvation and structural characteristics of charged surfactants adsorbed at an interface has been the focus of many theoretical and experimental studies ranging from simple surfactants such as sodium dodecyl sulfate (SDS) to more complex and biologically relevant surfactants, lipids.[3−10]

In an effort to gain insight into the structure and bonding properties of water solvating the ionic portion of organized assemblies of charged surfactants at aqueous boundaries, studies by Gragson and Richmond[9,10] employed vibrational sum-frequency spectroscopy (VSF). These studies demonstrate how charged surfactant monolayers influence the orientation, hydrogen bonding, and structure of interfacial water as a function of surface charge and surface charge density. The results revealed that at high surfactant surface densities, a large uniform electric field gradient extends ∼100 Å into the bulk aqueous phase, orients a large volume of H_2O molecules, and enhances the tetrahedral bonding structure between neighboring H_2O molecules. Unfortunately, these studies were unable to capture the aqueous solvation of trace concentrations of charged surfactants adsorbed at the interface and the gradual buildup of surface charge, beginning with single molecular ion solvation. Hence, their studies primarily focused on the OH stretching characteristics of the water in the double layer region created by the charged surfactant monolayer and counterions in solution. Although theoretical examination of single surfactant solvation at the liquid/liquid interface has been performed,[4] direct experimental measurements are virtually nonexistent. Studies described herein present the first spectroscopic measurement of water molecules solvating charged surfactants at surface densities corresponding to isolated surfactant solvation. These studies also examine the water structure at surfactant surface densities such that interactions between adjacent surfactants and their solvation shells are no longer negligible.

The principal experimental method employed in these studies is vibrational sum-frequency spectroscopy.[11−14] Vibrational spectroscopic techniques are valuable for exploring the molecular environment of water at surfaces because H_2O vibrational modes are sensitive to the variation of H-bonding interactions that occurs between water molecules in distinct molecular environments.[15,10,16] The specificity of the second-order VSF process to molecules residing in the anisotropic environment of the interfacial region make it well suited for studies at the liquid/liquid interface.[11]

The studies described herein examine VSF spectra of interfacial water as trace surfactant concentrations of dodecyltrimethylammonium chloride (DTAC) and sodium dodecyl sulfate (SDS) adsorb at the CCl_4/H_2O interface. At trace concentrations, the area available to each interfacial surfactant is much larger than the molecular dimensions and the system can be characterized as a two-dimensional gaseous film of charged surfactants. Experimental results will show that a gaseous film of charged surfactants produces dramatic changes to the vibrational spectrum of neat interfacial water. Spectral changes are attributed to solvating H_2O influenced by the electric fields that arise from the charged headgroup and counterion. These strong charge−dipole interactions act to orient solvating water molecules in both the organic and aqueous regions of

* To whom correspondence should be addressed. E-mail: richmond@darkwing.uoregon.edu.

10.1021/jp048378x CCC: $27.50
Published on Web 07/28/2004

the interface. The electric-field-induced effects result in large enhancements to the VSF response from solvating water molecules and makes it possible to distinguish the spectrum of these water molecules from the more prevalent interfacial molecules unperturbed by the surfactant. Results indicate that these solvating water molecules are preferentially oriented and have peak positions and spectral widths indicative of weaker hydrogen bonding interactions than those observed in bulk liquid water. In addition to the trace surfactant surface concentration studies, a series of concentrations are presented that follow the evolution of the interfacial water spectrum as surfactant concentrations are increased to a level where collective interaction between water molecules and surfactants increase. Stronger H_2O-H_2O interactions become increasingly apparent with augmented surfactant surface concentrations.

VSF Background

Vibrational sum frequency generation is a surface specific nonlinear optical technique employed to obtain vibrational spectra of interfacial molecules and is defined as the coherent coupling to two photons (ω_1 and ω_2) that produce a single photon (ω_3) at the sum of their two frequencies ($\omega_3 = \omega_1 + \omega_2$).[17,18] The intensity ($I(\omega_{SF})$) of the sum frequency response is described by the second-order term in the expansion of the macroscopic polarization of a dielectric medium and is proportional to eq 1,[19−22]

$$I(\omega_{SF}) = |P_{SFG}|^2 \propto |\chi_{NR}^{(2)} + \sum_{\nu}\chi_{\nu}^{(2)}|^2 I(\omega_{IR})I(\omega_{vis}) \quad (1)$$

where P_{SFG} is the second-order polarization, $\chi_{NR}^{(2)}$ and $\sum_{\nu}\chi_{\nu}^{(2)}$ are the nonresonant and resonant second-order nonlinear susceptibility tensors respectively, which describe the nonlinear response of the medium to the intensity of the two radiation fields $I(\omega_{IR})$ and $I(\omega_{vis})$. For these studies in which a nanosecond laser is employed at a liquid/liquid surface the nonresonant contribution is negligible.

The dominant contribution to the detected VSF intensity arises from the resonant contribution

$$\chi_{\nu}^{(2)} \propto \frac{A_{\nu}}{\omega_{IR} - \omega_{\nu} + i\Gamma_{\nu}} \quad (2)$$

which is summed over all SF active vibrational modes. The terms ω_{IR} and ω_{ν} correspond to the frequencies of the IR radiation and molecular vibrational transition, respectively. Γ_{ν} is the natural line width of the transition and A_{ν} is the amplitude coefficient proportional to the product of the Raman and IR transition moments.

When a uniform charge is located at an interface the influence of the static electric field (E_0) can contribute to the additional alignment of interfacial and bulk molecules containing a dipole, such as H_2O. This alignment effectively extends the region of anisotropic forces into the bulk liquid and produces a third-order ($\chi^{(3)}$) contribution to the nonlinear polarization as follows:[23−26,10]

$$P_{SFG} = \chi^{(2)}{:}E_{vis}E_{IR} + \chi^{(3)}{:}E_{vis}E_{IR}E_0 \quad (3)$$

The second term in eq 3 is the third-order polarization and similar to $\chi^{(2)}$; $\chi^{(3)}$ can also be separated into resonant and nonresonant contributions. In the case of aqueous interfaces, the magnitude of the third-order polarization induced by the static electric field is determined by the electronic nonlinear polarizability (deformation polarizability) of water, the degree of alignment of water molecules (orientation polarizability), and the magnitude of the static electric field.[25,27] At aqueous interfaces in the presence of a monolayer of charged surfactant, it has been observed that the third-order resonant contribution to the polarization is dominated by the orientation polarizability, due to the large number of bulk H_2O molecules that are aligned by the penetration of the electric field E_0 into the bulk solution. The alignment of interfacial and additional bulk H_2O molecules is observed in VSF experiments as a large enhancement in SF signal in the OH stretching region.[28,10,29,30]

In addition to measuring the vibrational spectra of interfacial molecules, VSF can be employed to ascertain molecular orientation with the judicious choice of polarizations for SF, visible, and IR radiation, which access different components of the $\chi^{(2)}$ tensor.[20] Experiments described herein have been performed by collecting SF radiation under *s*,*s*,*p* polarization conditions (*p*-polarization and *s*-polarization are defined as parallel and perpendicular to the plane of incidence, respectively), which refer to the polarizations of SF, vis, and IR radiation, respectively. Under $I_{s,s,p}$ polarization conditions, experiments access vibrational modes with a component of their transition dipole normal to the interfacial plane. $I_{s,p,s}$ and $I_{p,s,s}$ measure the in-plane dipole response.

Due to the coherent nature of VSF spectroscopy each vibrational band exhibits an inherent phase for a fixed molecular orientation and this phase is expressed as the + or − sign in conjunction with the fitted amplitudes. Variation of phase occurs with an orientational change.[31,13] The overlapping of vibrational modes of opposite or congruent phases leads to spectral interferences and contributes to the asymmetric character of overlapping vibrational bands in VSF spectra.[32] Accurate spectral modeling of these interference effects not only renders differing interfacial H-bonding environments in the case of H_2O but also information on molecular orientation. A detailed description of the spectral fitting method is beyond the scope of this article but is the focus of an earlier publication by Brown et al.[31]

Experimental Section

The laser system employed in these studies has been described in detail elsewhere.[33] Briefly, it consists of an Nd:YAG diode seeded laser that pumps a double pass optical parametric oscillator/optical parametric amplifier in series producing mid-infrared radiation tunable from ∼ 2.5−4 μm. The mid-infrared pulse energies employed at the experiment range from of approximately 2 mJ at 2.5 μm to 1 mJ at 4 μm with a bandwidth of ∼1 cm^{-1}. The mid-infrared pulses are overlapped spatially and temporally at the interface with 532-nm radiation generated in a BBO crystal. Nearly 90% of the IR path length is contained within an atmosphere that is circulated over activated charcoal and anhydrous calcium sulfate to remove atmospheric water vapor. IR adsorptions by rovibrational bands of residual water vapor are responsible for sharp (1−4 cm^{-1} FWHM) intensity dips in SF spectra between 3550 and 3800 cm^{-1}.

The CCl_4/H_2O experiments have been performed using a Kel-F cylindrical cell that is placed on top of an IR grade quartz prism. Doubly distilled CCl_4 (Aldrich, 99.9% HPLC grade) was placed in the cell and covered with H_2O (Mallinckrodt ChromAR HPLC Grade)/surfactant solution. The collimated (∼1 mm) *s*-polarized 532-nm radiation is coupled into the cell through the prism at the critical angle (66° from the surface normal). As the 532-nm radiation passes from the high index medium (CCl_4: $n^{20} = 1.4607$) to the low index medium (H_2O: $n^{20} = 1.3330$) it is totally internally reflected (TIR) at the CCl_4/

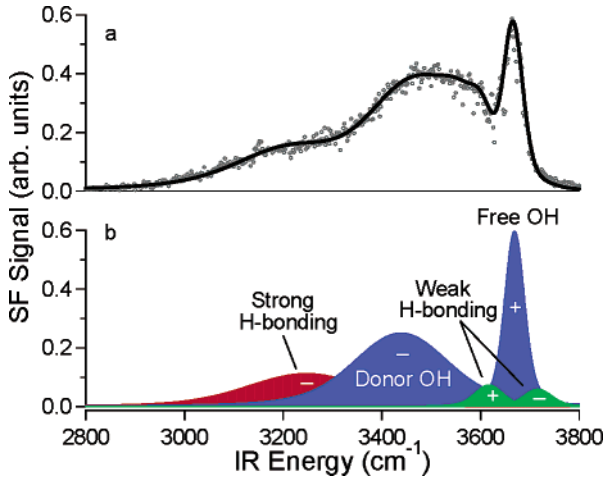

Figure 1. a. VSF spectrum of H_2O at the neat CCl_4/H_2O interface with the least-squares fit to the data superimposed as a solid line. Peak parameters are displayed in Table 1. b. Composite peaks for the various OH modes derived from the fit to the data.

H_2O interface.[34] Under TIR conditions sum-frequency signal is enhanced by several orders of magnitude over an externally reflected geometry and allows for the detection of low-SF water signal levels.[35−37] The *p*-polarized IR radiation is coupled into the cell at an angle of ∼73° to the surface normal in a copropagating configuration. The IR beam diameter incident on the interface was approximately 500 μm. The thickness of the CCl_4 layer was adjusted such that the IR path length was minimized in order to reduce IR absorption by monomeric H_2O within the CCl_4 phase. The 532 nm and IR radiation are overlapped at the CCl_4/H_2O interface and the *s*-polarized SF radiation collected on reflection. SF radiation is collected by a PMT, gated electronics, and computer. Each VSF CCl_4/H_2O spectrum is obtained with an increment of 2 cm^{-1} and an average of 50−100 pulses per increment. All spectra were obtained at room temperature. For a more complete description of the experimental setup employed in these experiments please refer to previous publications.[38,33]

dodecyltrimethylammonium chloride from TCI America, 98% d_{25}-sodium dodecyl sulfate, and *d*-ethanol from Cambridge isotope laboratories were used as received. Nanomolar aqueous concentrations of both DTAC and SDS solutions were made by serial dilutions of micromolar stock solutions. Aqueous surfactant solutions were added to the experimental cell over the CCl_4 phase and allowed to equilibrate. Surfactant adsorption to the interface and equilibration of the CCl_4/H_2O/surfactant system and was followed by temporally monitoring the VSF signal increase/decrease in the OH-stretching spectral region. All glassware and sample cells were soaked in concentrated sulfuric acid containing No-chromix to remove any organics and surface-active contaminants. After removal from concentrated acid, equipment was thoroughly rinsed with 17.9 MΩ water from a Nanopure filtration system until free from acid residue.

Results and Discussion

Water Structure at the Neat CCl_4/H_2O Interface. The VSF spectrum of interfacial water at the CCl_4/H_2O interface has been measured previously and is displayed in Figure 1a. The results are briefly described here because of their relevance to the surfactant results described later. The least-squares fit to the data, superimposed as the solid line (Figure 1a), and a detailed assignment of contributing peaks (Figure 1b) are described in previous publications.[33,38] Table 1 summarizes the assignments and derived peak parameters.

TABLE 1: Fit Parameters and Orientations Determined for theCCl_4/Water System[a]

	frequency (ω_ν/cm^{-1})	width (FWHM/ cm^{-1})	amplitude (A_ν)	orientation
	interfacial H_2O			
ν_1 (symmetrically bonded)	3247	142	−0.34	$\theta > 90°$
donor OH	3439	113	−0.51	$\theta > 90°$
ν_1 monomeric/ HB acceptor	3617	33	0.29	$\theta < 90°$
free OH	3669	23	0.85	$\theta < 90°$
ν_3 monomeric/ HB acceptor	3716	33	−0.26	$\theta > 90°$

[a] Results from the least-squares fit to the VSF data collected for H_2O at the neat CCl_4/H_2O interface (Figure 1a). The amplitude of the free OH vibration is assigned a positive value (phase) consistent with the dipole orientation pointing toward the aqueous phase. The positive/negative sign associated with each amplitude parameter reflects the phase of a particular molecular vibration. θ is defined as the angle between the symmetry axis of the H_2O molecule and the Z axis of the laboratory frame. The Z axis lies normal to the interfacial plane and $\theta = 0°$ describes an H_2O molecule oriented such that the molecular dipole points toward the aqueous phase.

The spectral envelope of H_2O at the CCl_4/H_2O interface contains OH stretching modes for interfacial water molecules in three distinct hydrogen bonding environments: (1) strongly H-bonded tetrahedrally coordinated H_2O, (2) intramolecularly uncoupled H_2O that straddles the interface, and (3) monomeric/hydrogen bond (HB) acceptor H_2O. The peak at 3247 cm^{-1} corresponds to the symmetric stretch (ν_1) of the most strongly H-bonded water molecules observed at this interface. These H_2O molecules participate in energetically symmetric H-bonding interactions, therefore retaining the C_{2v} symmetry. This peak represents the only water molecules at the CCl_4/H_2O interface found to be tetrahedrally coordinated. Contributing water molecules are oriented such that the molecular dipole is on average pointing normal to the interfacial plane and in the direction of the CCl_4 phase, with the dipole defined as pointing from electropositive to electronegative (i.e., with hydrogens pointing toward the H_2O phase). The two peaks at 3439 and 3669 cm^{-1} correspond to water molecules that straddle the interface. The free OH bond (3669 cm^{-1}) is oriented into the CCl_4 phase and is vibrationally uncoupled from the intramolecular OH donor bond (3439 cm^{-1}) that is predominately in an aqueous phase environment. The peaks at 3617 and 3716 cm^{-1} correspond to the symmetric (ν_1) and asymmetric (ν_3) stretching modes of interfacial water molecules participating in very weak H-bonding interactions at their proton sites. These peaks represent interfacial H_2O that are either completely surrounded by CCl_4 molecules (monomeric H_2O) or interact with neighboring water molecules solely through electron donor interactions, typically labeled hydrogen bond acceptor (HB acceptor H_2O).[33,39]

These five fitted peaks constitute the dominant features giving rise to the VSF spectral envelope obtained for H_2O at the neat CCl_4/H_2O interface under $I_{s,s,p}$ polarization conditions. The results signify that weak H-bonding and less-than-tetrahedral coordination persist perpendicular to the interface. Although complicated by CH stretching modes that adsorb incident IR radiation in the 2800−3200 cm^{-1} region, hexane/H_2O and hexene/H_2O systems also exhibit similar spectral features in the 3500−3700 cm^{-1} region that indicate weak H-bonding interactions are prevalent at these organic/water interfaces.[40,33,38]

Interfacial Water Structure in the Presence of a Monolayer of SDS. When a monolayer of charged surfactant adsorbs

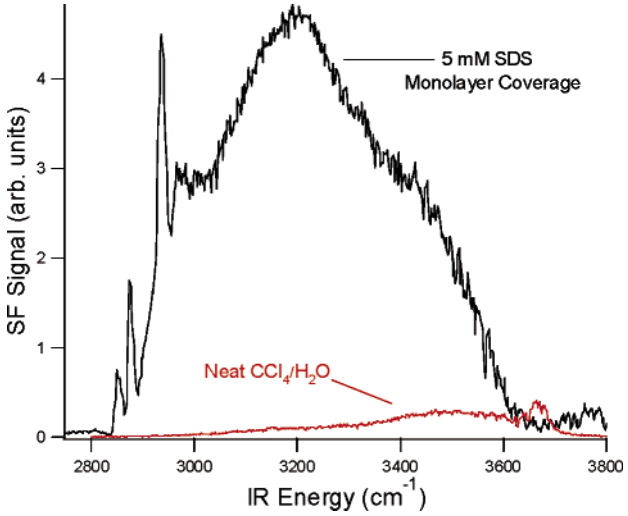

Figure 2. VSF spectrum of the CCl_4/H_2O interface at monolayer coverage of SDS displayed with the VSF spectrum of the neat CCl_4/H_2O interface from Figure 1. Comparison of the two VSF spectra indicate the distinct differences in hydrogen-bonding environments at the CCl_4/H_2O interface in the presence and absence of a charged surfactant monolayer.

at the water surface, whether it be vapor/water or organic/water interface, the surface water spectrum changes dramatically.[10] Figure 2 displays a VSF spectrum of the CCl_4/H_2O interface with a saturated monolayer of negatively charged surfactant (SDS) adsorbed at the interface. Prominent OH stretching features of water are observed near 3200 and 3400 cm^{-1}, consistent with earlier studies of the CCl_4/H_2O/surfactant interface by Gragson et al.[9] using a picosecond laser system. The sharp spectral features located between ~2850 cm^{-1} and ~2950 cm^{-1} originate from the CH stretching modes associated with the long alkyl chain ($C_{12}H_{25}$) of the surfactant. For comparison, Figure 2 also contains the neat CCl_4/H_2O VSF spectrum. This overlay compares the interfacial water structure and hydrogen bonding in the presence and absence of a uniform surface charge, as measured by the OH stretching modes of interfacial H_2O. The most obvious differences are the significantly large increase in OH intensity, red-shifted OH peak frequencies, and extinction of the free OH mode with adsorption of SDS to the interface. These spectral differences are the result of changes to the hydrogen bonding and structure of water molecules influenced by the large electrostatic fields (10^7 V/m) imposed by the uniform distribution of charged headgroups situated in the aqueous phase of the interfacial region. The electrostatic field is understood to align interfacial water molecules beyond the first few water layers and therefore extend the asymmetry of the interfacial region into the bulk aqueous phase. The electric field therefore has a twofold effect on the intensity of observed OH oscillators. In addition to aligning the H_2O dipole normal to the interfacial plane, which in turn augments the intensity of the generated SF under *s,s,p* polarization conditions, the electric field gradient also increases the number of contributing water molecules by increasing the depth of the interfacial region. The observed increase in cooperative bonding between H_2O molecules as a result of an applied electric field has also been reported in previous spectroscopic[29,10,9,41] and theoretical studies.[42] Consequently, strong vibrational coupling between water molecules contributes to increased intensity and red-shifted OH oscillator peak frequencies[39,43] that are apparent with monolayer adsorption of SDS at the neat CCl_4/H_2O interface (Figure 2). Experiments by Gragson et al.[9] were not performed at concentrations examined herein and thus the large SF signal from water molecules in the double layer region limited the examination of the much smaller signal resulting from the lesser number of water molecules that directly solvate the ionic headgroup of the surfactant.

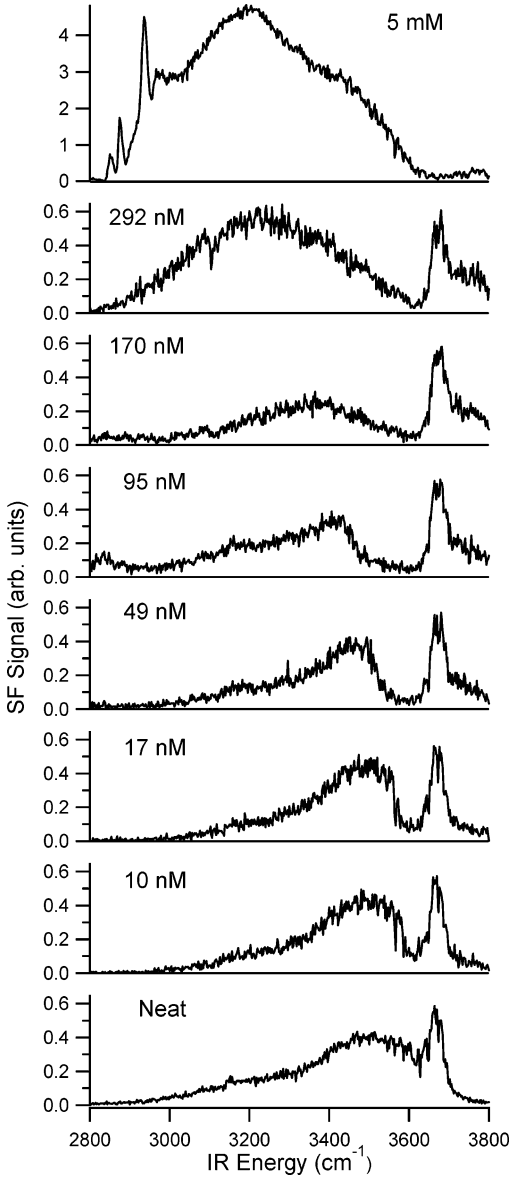

Figure 3. VSF spectra of H_2O at the CCl_4/H_2O interface for a series of bulk aqueous phase concentrations of d_{25}-sodium dodecyl sulfate under $I_{s,s,p}$ polarization conditions. The topmost spectrum corresponds to monolayer coverage of nondeuterated SDS.

Gaseous Surfactant Films at the CCl_4/H_2O Interface. To uncover spectral contributions due to water molecules directly solvating the surfactant headgroup, VSF experiments were conducted at interfacial concentrations where interactions between neighboring surfactants and their solvation shells are negligible. Surface pressure measurements performed at the CCl_4/H_2O/surfactant interface have been employed to characterize the surfactant interfacial concentration and direct spectroscopic experiments to the appropriate surfactant concentration range (nanomolar bulk aqueous phase concentrations). The following paragraphs will focus on the qualitative spectral changes and a more detailed spectral analysis will follow in the proceeding sections.

Anionic Surfactant. Figure 3 displays VSF experiments performed at the CCl_4/H_2O interface for a series of nanomolar (nM) aqueous phase concentrations of sodium dodecyl sulfate

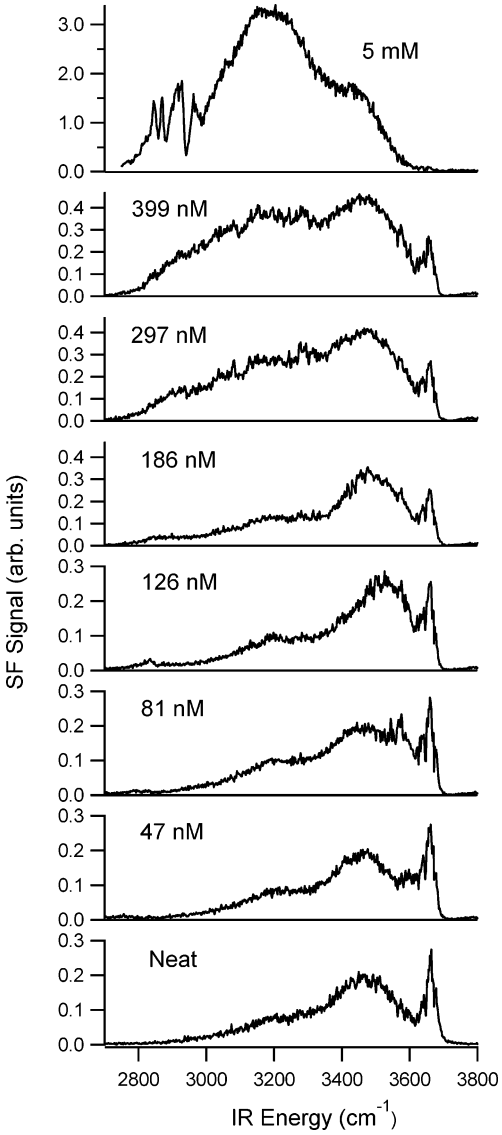

Figure 4. VSF spectra of H_2O at the CCl_4/H_2O interface for a series of bulk aqueous phase concentrations of dodecyltrimethylammonium chloride under $I_{s,s,p}$ polarization conditions. The topmost spectrum corresponds to monolayer coverage of DTAC.

(SDS). At a bulk aqueous concentration of 10 nM SDS, a sharp dip in intensity occurs near 3600 cm^{-1}. As the concentration of SDS is increased from 17 nM to 95 nM SDS the dip in intensity that began at ~3600 cm^{-1} becomes more pronounced and extends as far as the 3500 cm^{-1} region. When concentrations near 170 nM SDS, the spectral changes observed in the 3500−3600 cm^{-1} of the OH stretching region cease. The spectral intensity near 3200 cm^{-1} begins to increase as the concentration reaches 292 nM and the vibrational profile of H_2O begins to resemble that observed at monolayer coverage of SDS (Figure 2 and Figure 3 topmost panel), where the uniform surface charge promotes alignment and increased H-bonding interactions between neighboring interfacial water molecules.

*Cationic Surfactant***.** Figure 4 displays VSF experiments performed at the CCl_4/H_2O interface for a similar concentration series of dodecyltrimethylammonium chloride (DTAC). At an aqueous concentration of 47 nM DTAC, adsorption of the cationic surfactant at the interface produces a narrow band of spectral intensity near 3600 cm^{-1}. This trend with concentration continues as the DTAC concentration is increased to 81 nM. When DTAC concentrations reach 126 nM there are visible spectral changes in the 3500 cm^{-1} region of the spectrum and these changes cease at ~200 nM. Further increases in DTAC concentration to 297 nM and 399 nM promote broad intensity increases near 3200 cm^{-1}, similar to those changes seen in the SDS series above ~200-nM bulk aqueous concentration.

Though the spectral regions influenced by the adsorption of both anionic and cationic surfactants to the interface at bulk aqueous concentrations below ~200 nM are similar, the observed changes in spectral intensity of these regions exhibit an inverse behavior. The inverse H_2O spectral changes observed for the oppositely charged surfactants represents the difference in orientation of the probed solvating water molecules caused by the electrostatic field orientation. What is most interesting about these results is that the concentration series clearly show that particular regions of the H_2O spectrum are changing at specific concentration ranges. For example, at the lower end of the SDS concentration series (<20 nM), spectral changes are localized in the spectral region (3600 cm^{-1}) to the red of the free OH oscillator peak (3669 cm^{-1}), a region indicative of water molecules participating in relatively weak hydrogen bonding interactions. As the surfactant concentration increases toward ~200 nM, the spectral changes become much broader and encompass ~ 3450−3600 cm^{-1}. Spectral intensity in this region is indicative of a more disorganized hydrogen-bonding network relative to bulk liquid water. Spectra at concentrations greater than ~200 nM display broad intensity increases at ~3250 cm^{-1}, a spectral signature of bulk liquid H_2O molecules participating in a relatively strong and highly correlated hydrogen-bonding network. The same trend is also observed for the DTAC series.

Although there are significant spectral changes to the OH stretching region of interfacial water molecules, the free OH oscillator intensity and frequency remain relatively constant at concentrations below ~200 nM for both cationic and anionic surfactant. This behavior, in addition to surface pressure measurements described below, suggests that a significant fraction of the interface is void of perturbations caused by the adsorption of the charged surfactant to the interface. This also indicates that observed OH spectral changes emanate from a small number of water molecules solvating well-separated and noninteracting surfactant molecules at the CCl_4/H_2O interface. At concentrations above ~200 nM the free OH intensity begins to diminish.

In summary, the concentration-dependent spectral changes described above show the variation in solvating water structure as the surfactant surface concentration is increased from trace concentrations, where interactions between adjacent solvation shells is negligible (single molecular ion solvation at an interface), to a structure governed by the partial overlapping solvation shells and a large uniformly penetrating electric field.

Surface Concentration Measurements

Surface pressure measurements performed at the CCl_4/H_2O/surfactant interface employing the Wilhelmy plate method[1] provide insight into the level of interfacial surfactant concentrations responsible for the observed spectral changes. Surface pressure verses bulk surfactant concentration measurements relate thermodynamic surface pressure data to a quantitative measure of surfactant surface density (Å^2/surfactant molecule). Results of surface pressure versus surfactant bulk concentration measurements collected at the CCl_4/H_2O/SDS interface by Conboy et al.[6,34] indicate SDS monolayer coverage occurs near 2-mM bulk aqueous concentration with a limiting surface density of 59 Å^2/molecule (88 Å^2/molecule DTAC). The VSF spectra of H_2O corresponding to monolayer coverage is displayed in

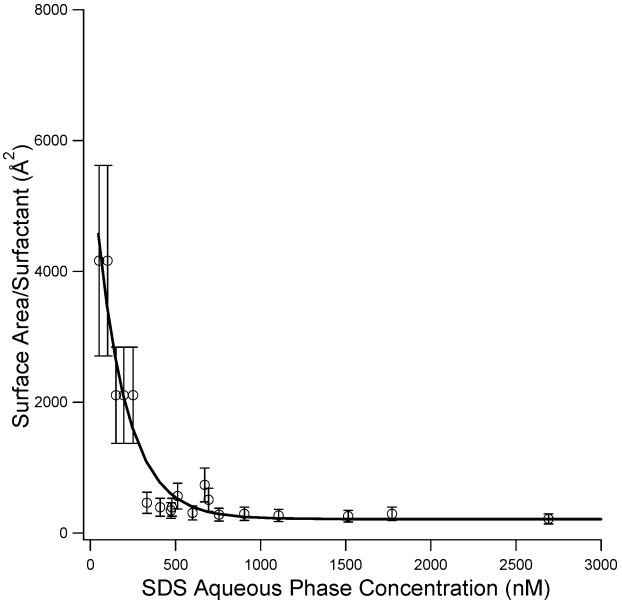

Figure 5. Plot of SDS surface densities at the CCl_4/H_2O interface versus the SDS bulk aqueous phase concentration. The solid line is shown as a guide to the eye.

Figure 2 (SDS), and in the topmost panels in Figures 3 (SDS) and 4 (DTAC). At aqueous phase concentrations below 2 mM SDS, surface area increases to near 500 Å^2 at 500 nM SDS. Similar surface areas are observed for DTAC at ~500-nM concentration. The VSF spectroscopy of interfacial water molecules at these intermediate concentrations of SDS and DTAC (500−2 mM) are the topic of previous publications by Gragson et al.[9,10] Figure 5 displays the experimental results of Wilhelmy plate surface pressure measurements performed by this lab in the form of surfactant surface density versus bulk aqueous concentration of SDS in the nanomolar concentration range. Below ~500 nM SDS bulk aqueous concentration, surface pressure measurements indicate rapidly decreasing surface densities with small decreases in the surfactant concentration. At 50 nM SDS, surfactant surface areas approach ~4000 Å^2/surfactant molecule. Although surface pressure measurements at these low surfactant concentrations (<500 nM) contain significant uncertainties, the ideal gas law modified for a two-dimensional gaseous surfactant film[44] produces similar surface areas. Based on the surface pressure measurements presented above we conclude that the average surface area for SDS and DTAC range from ≫4000 Å^2/molecule at 10 nM to near 500 Å^2/molecule at 500 nM surfactant aqueous concentration.

Surface pressure measurements thus indicate that spectral changes observed at surfactant concentrations below ~200 nM in Figures 3 and 4 evolve from water molecules that essentially solvate *isolated* surfactant molecules adsorbed at the CCl_4/H_2O interface. Consequently, H_2O spectral contours at concentrations <200 nM in Figures 3 and 4 are the convolution of two distinct VSF spectra: (1) the neat interfacial spectrum shown in the bottom panel of Figures 3 and 4, and (2) the vibrational spectrum of a volume of solvating water molecules perturbed by the electric field emanating from an isolated charged surfactant and counterion situated in the interfacial region. The spectral fitting procedure described below is developed from this low concentration model.

Spectral Analysis

Trace Surfactant Concentrations. The topmost panels of Figures 6a, b, and 7 display the least-squares fit to the VSF

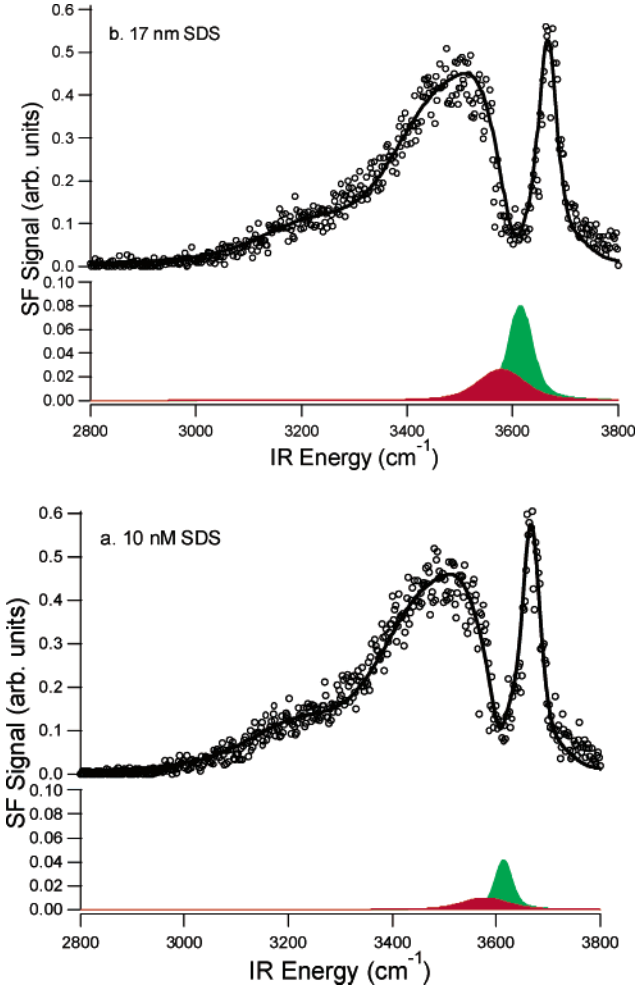

Figure 6. a. VSF spectrum of the CCl_4/H_2O interface at 10-nM concentration SDS. b. VSF spectrum of the CCl_4/H_2O interface at 17-nM concentration SDS. The least-squares fit to the data superimposed as a solid line. Peak parameters are displayed in Table 2. Spectral features contributing to the observed spectral changes and assigned to solvating H_2O molecules are shown below the corresponding fit to the spectral data. The shading of the solvation peaks corresponds to the water molecules displayed in Figure 8 with similar shading.

data obtained at the CCl_4/H_2O interface for bulk aqueous concentrations of 10 nM, 17 nM SDS, and 47 nM DTAC, respectively. To determine the spectral profiles for solvating water molecules, the best fits to the data were generated by first attaining a least-squares fit to the neat CCl_4/H_2O VSF spectral envelope, corresponding to the bottom-most spectrum in the SDS and DTAC experimental series (Figure 3, 4). This initial fitting procedure determines the various contributions (Figure 1b) to the neat CCl_4/H_2O data that will be subsequently applied to the fits of the SDS (10 nM, 17 nM) and DTAC (47 nM) VSF data. Next, best fits to the 10 nM, 17 nM SDS, and 47 nM DTAC data are generated by combining the spectral contributions from the neat CCl_4/H_2O spectral fit and a minimum number of additional peaks. These new additional peaks represent the OH stretching modes of water molecules solvating the surfactant headgroup. The lower panels of Figure 6a, b, and 7 display the peaks assignable to solvating water molecules for 10 nM, 17 nM SDS, and 47 nM DTAC. Spectral parameters for solvating water molecules derived from the fit to the spectral data are summarized in Table 2.

We view these solvating water molecules as either directly hydrating the charged surfactant headgroup (primary (1°) solvation shell) or water molecules not directly interacting with

TABLE 2: Fit Parameters and Orientations Determined for the CCl_4/Water/Surfactant System[a]

concn (nM)	frequency (ω_ν/cm^{-1})	width (FWHM/cm^{-1})	amplitude (A_ν)	orientation
		DTAC		
47	3586	40	−0.13	$\theta > 90°$
	3615	20	0.07	$\theta < 90°$
		SDS		
10	3579	50	0.11	$\theta < 90°$
	3615	17	−0.28	$\theta > 90°$
17	3579	50	0.18	$\theta < 90°$
	3615	25	−0.35	$\theta > 90°$

[a] Results from the nonlinear least-squares fit to the data collected for H_2O at the CCl_4/H_2O interface at aqueous concentrations of 10 nM, 17 nM SDS (Figure 6a, b), and 47 nM DTAC (Figure 7). Each of the three fit spectral peaks for both SDS and DTAC are responsible for the VSF spectral contour changes that occur to the neat CCl_4/H_2O VSF spectrum. The amplitude of the free OH vibration is assigned a positive value (phase) consistent with the dipole orientation pointing toward the aqueous phase. The positive/negative sign associated with each amplitude parameter reflects the phase of a particular molecular vibration.

the headgroup (secondary (2°) solvation shell) but are perturbed by the emanating electric field.[45] The fitted solvation peaks of Figure 6a, b, and 7 share several common attributes: (1) they are located in the OH stretching region above 3500 cm^{-1} and therefore result from water molecules participating in relatively weak hydrogen bonding interactions at their proton sites, (2) the contributing peaks for the anionic surfactant (SDS) have similar peak frequencies, 3579 ± 4 cm^{-1} and 3615 ± 3 cm^{-1}, to those observed for the case of the cationic surfactant (DTAC), 3586 ± 3 cm^{-1} and 3615± 3 cm^{-1}. Although both cationic and anionic surfactants contain two contributing spectral features with similar peak frequencies, the resulting effect on the VSF spectral contour of H_2O is strikingly different and suggests that inherent differences in solvation occur with oppositely charged surfactants.

The peak at 3615 cm^{-1} for both charged surfactants is attributed to the coupled ν_1 stretching mode of weakly interacting (monomeric and/or HB acceptor) water molecules that lie in the CCl_4-rich portion of the interface. This assignment is facilitated by spectral similarity of these peaks with those assigned to monomeric/HB acceptor water molecules in the neat CCl_4/H_2O studies (Figure 1, 3617 cm^{-1}). These water molecules participate in weak interactions with the surrounding CCl_4 molecules and display a charged dependent orientation manifested in the peaks' relative phase derived from the spectral fit. The negative amplitude of the 3615 cm^{-1} (ν_1) peak for SDS denotes the average molecular dipole vector orientation of H_2O pointing in the direction of the CCl_4 phase (H atoms directed toward the aqueous phase). The dip in intensity near 3600 cm^{-1} (Figure 6a, b) is therefore a consequence of destructive interference between the peak at 3615 cm^{-1} and adjacent vibrational modes. Conversely, the positive amplitude of the analogous peak for DTAC indicates an opposite orientation and hence produces constructive interference with neighboring vibrational modes near 3600 cm^{-1} (Figure 7).

Although the peak at 3615 cm^{-1} is observed to approach a near-180° orientational difference for cationic and anionic surfactants, the peak frequency stays constant, an indication that these solvating H_2O molecules maintain minimal interactions at their proton sites with neighboring H_2O or CCl_4 molecules (i.e., do not participate in hydrogen-bond donating interactions). Similar orientation effects have been seen in pH studies of the neat CCl_4/H_2O interface.[33] Figure 8 depicts these solvating water

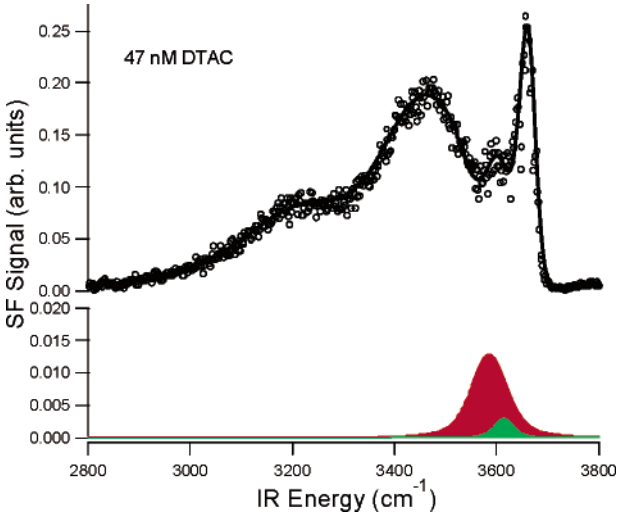

Figure 7. VSF spectrum of the CCl_4/H_2O interface at 47-nM concentration DTAC with the least-squares fit to the data superimposed as a solid line. Peak parameters are displayed in Table 2. Spectral features contributing to the spectral changes and assigned to solvating H_2O molecules are shown below the fit to the spectral data. The shading of the solvation peaks corresponds to the water molecules displayed in Figure 8 with similar shading.

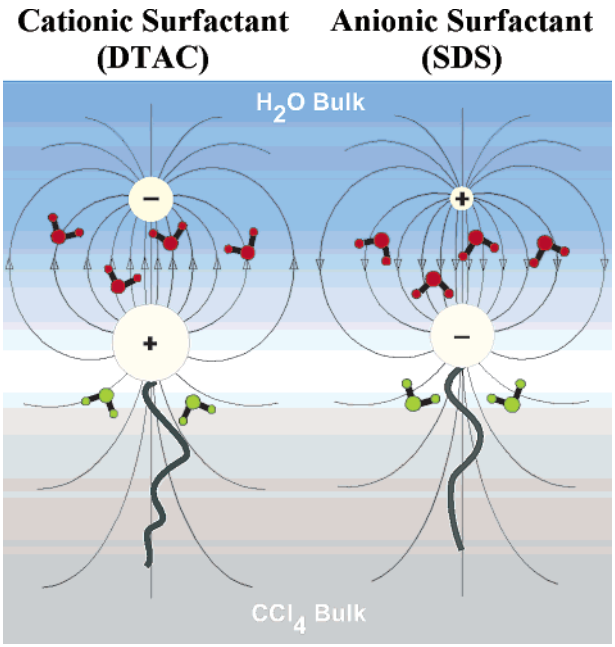

Figure 8. Schematic of solvating H_2O molecules displaying charge-dependent orientation due to charge−dipole interactions with anionic and cationic surfactants adsorbed at the CCl_4/H_2O interface. Water monomers in the CCl_4-rich side of the interface are oriented in opposite directions corresponding to the charge on the surfactant headgroup. Water molecules in the aqueous-rich side of the interface are similarly reoriented.

molecules that reside in the CCl_4 rich side of the interface and orient in response to charge-dipole interactions with the charged surfactants adsorbed at the interface.

The second contributing solvation peak determined from the spectral fit occurs near 3580 cm^{-1} (SDS = 3579 cm^{-1}, DTAC = 3586 cm^{-1}). These peaks lie in the spectral region indicative of water molecules participating in weak hydrogen-bonding interactions. Their peak frequencies are coincident with those observed in previous spectroscopic studies of solvating H_2O molecules in aqueous salt solutions and are in general agreement with frequency shift trends observed for halides and oxyanions

in aqueous solutions.[46−50] These studies demonstrate that the hydration of large oxoanions (ClO_4^-, ClO_3^-, and SO_4^{2-}) produce H_2O bond frequencies in the 3500−3600 cm^{-1} spectral region. The hydration of halides produces larger OH-bond red shifts near 3400−3500 cm^{-1} (Fl^-, Cl^-,Br^-, and I^-). The peak at 3579 cm^{-1} (SDS) correlates well with the above-mentioned salt studies, and is assigned to solvating H_2O molecules in an aqueous-rich environment around the SDS headgroup. Similarly, we assign the 3586 cm^{-1} peak (DTAC) to H_2O molecules solvating the cationic surfactant headgroup ($N(CH_3)_3^+$) in an aqueous environment. This assignment is based on the spectral similarities with the corresponding anionic surfactant peak and known charge−dipole and dipole−dipole interactions. When charge−dipole interactions are strong relative to dipole−dipole interactions, as in the case of water molecules hydrating an ion in solution, the tetrahedral bonding of H_2O molecules is partially broken down reducing the hydrogen bonding interactions between water molecules.[27] Although there will be an orientational difference between water molecules hydrating positively and negatively charged ions, hydrogen bonding interactions would be similarly weakened.

The near-180° phase difference between the 3586 cm^{-1} peak for DTAC and the 3579 cm^{-1} peak for SDS is represented by their negative and positive amplitude signs, respectively. This phase difference corresponds to a near-180° orientational difference that is reinforced by the fact that DTAC and SDS have oppositely charged headgroups. Figure 8 depicts water molecules on the aqueous-rich side of the interface displaying a charge-dependent orientation due to strong charge-dipole interactions with the surfactant at the interface. For DTAC, the negative amplitude sign associated with the 3579 cm^{-1} peak indicates that the molecular dipole for these water molecules is on average pointing toward the CCl_4 phase where the oxygen is oriented nearest the positively charged headgroup. This orientation is consistent with solvating water molecules on the aqueous-rich side of the surfactant headgroup. Conversely, SDS has a negatively charged headgroup and thus the lowest energy charge−dipole configuration of water molecules on the aqueous-rich side of the charged headgroup is with its molecular dipole oriented toward the aqueous phase. The positive amplitude sign determined for the ν_1 solvating peak of SDS at 3579 cm^{-1} indicates such an orientation.

In the previous discussion, we have neglected to comment on the spectral changes that take place to the blue of the free OH oscillator due to large experimental uncertainties at ∼3700 cm^{-1} of the VSF spectrum. This region of the H_2O vibrational spectrum has been assigned to the asymmetric stretching (ν_3, 3708 cm^{-1}) mode of H_2O molecules in a CCl_4 environment.[33,38,51,52] It is visually apparent that adsorption of SDS at the interface produces increased intensity in the 3700 cm^{-1} region of the spectrum while adsorption of DTAC to the interface produces a dip in intensity. Spectral fits to the data in a previously published letter[53] contain a peak near 3756 cm^{-1} for a good least-squares fit to the data. This peak has been omitted from the results published herein because of the large experimental uncertainties and because we obtain relatively good fit to the data in absence of this peak. Additional experiments are in progress to more definitively interpret this region of the spectrum.

To test the interpretation of the results for charged-surfactants, VSF experiments have also been performed using a nonionic surfactant (deuterated ethanol (CH_3CH_2OD)) adsorbed at the CCl_4/H_2O interface. Figure 9 displays the VSF spectrum of the CCl_4/H_2O interface at 224 μM bulk aqueous concentration of deuterated (OD) ethanol. Although the distinct appearance of the CH stretching modes in the 2850−2950 cm^{-1} region confirms the adsorption of ethanol at the interfacial region, the spectral changes observed in the 3600 cm^{-1} region with nanomolar concentrations of charged surfactants were not observed at 224-μM aqueous phase concentrations of ethanol. The adsorption of ethanol to the CCl_4/H_2O interface produces only small changes in the overall intensities of peaks assignable to water molecules that straddle the CCl_4/H_2O interface, namely, the intramolecularly uncoupled free (3669 cm^{-1}) and bonded (3439 cm^{-1}) OH stretches. Similar changes in the free OH stretch mode have been observed at the vapor/water interface with the adsorption of methanol to the interfacial region.[16] These results further support the conclusion that the OH spectral changes observed with isolated charged surfactants reflect the charge-dependent orientation and altered hydrogen-bonding environment of interfacial water molecules resulting from charge−dipole interactions imposed by the ionic headgroup and counterion in solution.

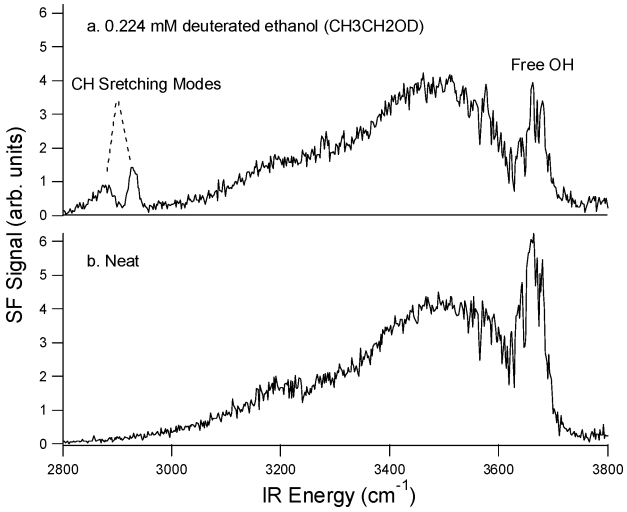

Figure 9. a. VSF spectrum of the CCl_4/H_2O interface at 224-μM bulk aqueous concentration of deuterated (OD) ethanol. b. VSF spectrum of the neat CCl_4/H_2O interface for comparison.

The fact that water molecules on the CCl_4 and H_2O-rich sides of the interface reorient in response to the charge on the interfacial surfactant molecules suggests that these water molecules lie within close proximity of the charged surfactant headgroup. It is therefore important to understand the strength and dimension of the electric fields created by the charged surfactant, which cause solvating water molecules in the H_2O and CCl_4-rich phases of the interfacial region to preferentially orient. A simple point charge model treating H_2O and CCl_4 as continuous liquids has been employed in order to calculate the charge−dipole interaction energy[54] and attain a quantitative description of the penetration depth and strength of the electric field with distance from the charged headgroup in solution. Figure 10 displays the charge−dipole interaction energy for a point dipole in both liquid water and liquid CCl_4 verses the distance from a point charge (r), where the dipole is oriented in its lowest energy position ($\theta = 0°$). As observed in the liquid H_2O curve, the relatively large dielectric constant of liquid water ($\epsilon_{H_2O} \approx 79$) attenuates the electric field over very short distances and is responsible for the sharp increase in interaction energy as separation is increased. The model suggests that at a distance of ∼2 Å thermal energy (kT) at room temperature begins to exceed the force of the charge-dipole interaction. Accounting for dielectric saturation,[27] which reduces the dielectric constant of water molecules to approximately $\epsilon_{H_2O} = 6$ in the primary

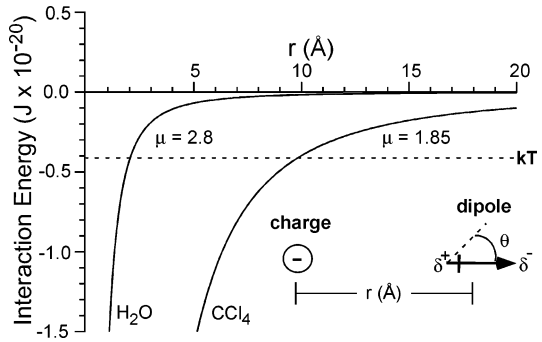

Figure 10. Plot of the charge−dipole interaction energy for a point dipole in both liquid H_2O and liquid CCl_4 versus the distance from the point charge. The dipole magnitude employed with liquid H_2O is 2.8 D and with liquid CCl_4 it is 1.85 D. The 2.8-D dipole represents an H_2O molecule participating in relatively strong H-bonding interactions with neighboring water molecules, similar to liquid water. The 1.85 D represents monomeric H_2O participating in very weak or negligible interactions with neighboring CCl_4 molecules.

solvation shell, the effective screening of the electric field will be reduced and consequently the depth of penetration will increase. This is consistent with molecular dynamics simulations of SDS at the CCl_4/H_2O interface at low surface coverage, where sulfate headgroup−water correlations persist beyond ~7 Å.[4] For the case of liquid CCl_4, the lack of a permanent dipole moment results in a relatively low dielectric constant ($\epsilon_{CCl_4} \approx 2$), thereby reducing the screening effect the CCl_4 phase has on the electric field. In this case, thermal energy begins to exceed the orienting effect of a charge at a distance of approximately 5 times the value calculated for liquid H_2O. Consequently, water molecules that penetrate or exist in the saturated (~10 mmole H_2O/L CCl_4)[55] organic phase are likely to be oriented to a dimension of several angstroms. Although a quantitative measure of the specific interfacial location and number of water molecules being examined cannot be ascertained within these experiments, the VSF technique probes those water molecules that are preferentially oriented by the penetrating field.

In summary, the results of the trace surfactant surface concentration experiments at the CCl_4/H_2O interface identify two types of interfacial water species that solvate the charged surfactant headgroup: (1) solvating water molecules on the CCl_4 rich side of the surfactant headgroup responsible for the ν_1 monomeric peak at 3615 cm^{-1}, in both SDS and DTAC experiments. Their corresponding phase factors are consistent with molecular orientations that produce the lowest charge−dipole interaction energy. (2) Solvating water molecules on the H_2O-rich side of the surfactant headgroup responsible for the ν_1 solvation peak near 3580 cm^{-1}. Their derived phase factors indicate opposing orientations corresponding to the charge on the headgroup and also opposing orientation to the monomeric H_2O molecules in the more CCl_4 rich phase.

Increased Surfactant Concentrations. As surfactant concentrations exceed those displayed in Figures 6 and 7, it becomes increasingly difficult to assign spectral features due to the appearance of broad overlapping and shifting spectral features in the OH stretching region. This is not unexpected given that IR and Raman spectra of bulk water are notoriously complex. It is more instructive and applicable at this point to analyze the spectral changes in a more qualitative manner as opposed to fitting the spectral data with an arbitrary set of spectral peaks to describe the data. Hence, the following discussion will focus on a qualitative description of the spectral changes that occur at concentrations exceeding 47 nM DTAC and 17 nM SDS concentrations. More detailed studies are in progress but are beyond the scope of this paper.

At trace (<50 nM) surfactant concentrations spectral features attributed to solvating H_2O are localized at ~3600 cm^{-1}. VSF spectra collected at slightly higher concentrations of charged surfactants (81−186 nM DTAC, 49−170 nM SDS) also exhibit significant spectral changes, although these changes are broader and more localized in the region near 3500 cm^{-1}. For 81−186 nM DTAC, surfactant adsorption at the interface produces a broad peak near 3500 cm^{-1} displaying negative amplitude and responsible for the observed constructive interference. At 49−170 nM SDS, evidence for a similar peak near 3500 cm^{-1} displaying positive amplitude is seen as a broad dip in intensity (destructive interference) centered near 3550 cm^{-1}. These dissimilar spectral changes for cationic and anionic surfactant are attributed to charge−dipole interactions that preferentially orient interfacial H_2O depending on the charge on the surfactant headgroup. Due to phase and frequency similarities with the fitted peaks at 3579 cm^{-1} (SDS) and 3586 cm^{-1} (DTAC) and spectral similarities with previously described aqueous salt solution studies, we conclude that the broad peak near 3500 cm^{-1} reflects solvating H_2O similarly oriented and experiencing slightly stronger hydrogen bonding interactions than those observed at trace surfactant concentrations.

Despite the occurrence of these broad spectral changes near 3500 cm^{-1} with increasing surfactant surface concentration, the free OH intensity and frequency remains relatively constant. The free OH oscillator is a good indicator of the degree of charged surfactant adsorption at the interface given that the free OH intensity diminishes and eventually disappears as more polar surfactants bond and cause the reorientation of these water molecules. We therefore conclude that although interfacial surfactant densities at these intermediate concentrations (81−186 nM DTAC, 49−170 nM SDS) produce relatively large spectral changes to the neat CCl_4/H_2O spectrum near 3500 cm^{-1}, a significant faction of interfacial H_2O molecules that straddle the interface are still unperturbed by the presence of surfactant.

As surfactant concentrations are increased to 297 nM DTAC and 292 nM SDS, increased intensity is observed near 3200 cm^{-1}, the region corresponding to tetrahedrally coordinated H_2O in a strongly hydrogen bonded environment. In fact, the vibrational contour of H_2O at these concentrations begins to resemble the VSF spectrum of H_2O at monolayer coverage (Figs. 3, 4, topmost panel), where the applied field promotes cooperative bonding between water molecules and increases the interfacial depth being probed. As the surfactant concentration approaches ~300 nM the distance between adjacent surfactants diminishes, and electrostatic and van der Waals forces no longer become negligible. Interfacial surfactants then begin to resemble a liquid expanded film and appear less like a gaseous film,[44,56] and VSF spectra show a corresponding change in water structure and hydrogen bonding with increasing intensity in the ~3200 cm^{-1} region. Consistent with this idea is the behavior of the free OH oscillator peak, which begins to display diminished intensity as the peak near 3200 cm^{-1} becomes more apparent. We attribute the behavior of the free OH oscillator at these surfactant concentrations to a reduction of the interfacial region unperturbed by surfactant-H_2O interactions. Surface pressure measurements described previously also support this interpretation and suggest that as charged surfactant concentrations near 500 nM, surfactant adsorption at the interface is decreased. This decrease in adsorption is attributed to increased surfactant surface densities and collective interactions between interfacial surfactants and solvating H_2O. Clearly the behavior of water at

the CCl_4/H_2O interface at charged surfactant concentrations near 300 nM is different and exhibits spectral features that are not observed at lower concentrations. Additional VSF experiments that probe the in plane response ($I_{s,p,s}$ polarization conditions) of interfacial OH modes are currently in progress to facilitate further characterization of H_2O structure and hydrogen bonding at the CCl_4/H_2O interface with increasing charged surfactant surface concentrations.

Summary and Conclusions

By virtue of examining the out-of-plane response of H_2O stretching modes at the CCl_4/H_2O interface, we have explored the hydrogen bonding, orientation, and structure of interfacial water with variation of surfactant charge and surface charge density. The difficult task of examining water buried at the liquid/liquid interface has been accomplished by employing vibrational sum-frequency spectroscopy, a technique that derives its surface selectivity from the intrinsic anisotropic environment of interfaces. VSF spectra of H_2O have been collected with anionic (SDS) and cationic (DTAC) surfactants adsorbed at the interface for a series of aqueous phase concentrations that result in a range of surfactant surface densities. Beginning at trace (<50 nM) surfactant concentrations, water solvating a two-dimensional gaseous film of positively and negatively charged surfactants is characterized. Observed spectral features can be attributed to monomeric water molecules residing in the CCl_4-rich side of the interface where H_2O-CCl_4 interactions are weak and produce sharp spectral features. In addition, water molecules residing in the aqueous-rich side of the interface have been observed and assigned by comparison to IR and Raman studies of water-solvating ions in solution, which produce broadened spectral features with similar frequencies. Manifested in the phase of assigned peaks, these solvating water molecules also exhibit charge-dependent orientation as a result of strong charge-dipole interactions between the surfactant headgroup and H_2O. As surfactant concentrations are increased, the progressive increase in surface charge density produces spectral features similar to those observed at monolayer coverage. The observed VSF spectroscopy trends in conjunction with surface pressure data strongly suggest that surfactant surface concentrations begin to resemble an expanded monolayer film as bulk aqueous phase concentrations near 300 nM.

These studies represent the first direct observation of water molecules hydrating the ionic portion of isolated surfactants adsorbed at a liquid/liquid interface. Systems such as the organic/water interface with an embedded isolated charge begin to uncover the molecular-level organic−water and ion−water interactions that govern many biological processes being studied at present. For instance, the interaction of an aqueous solvent with the polar and nonpolar units of proteins are responsible for processes such as protein folding and stabilization of the biological conformation. These studies also provide new insight into the effects of increasing surface charge density on the structure, hydrogen bonding, and orientation of interfacial H_2O at an organic/water interface. These results have important implications for developing a molecular-level picture of aqueous solvation of charge at an interface and understanding interfacial interactions that play a pivotal role in ion transport, macromolecular folding, and surfactant assembly.

Acknowledgment. The authors gratefully acknowledge the National Science Foundation (CHE-9725751) for funding these studies.

References and Notes

(1) Adamson, A. W.; Gast, A. P. *Physical Chemistry of Surfaces*, Sixth edition; John Wiley & Sons, Inc.: New York, 1997.
(2) Hills, B. A. *The Biology of Surfactant*; Cambridge University Press: New York, 1988.
(3) Schweighofer, K. J.; Essmann, U.; Berkowitz, M. *J. Phys. Chem. B* **1997**, *101*, 10775−10780.
(4) Schweighofer, K. J.; Essmann, U.; Berkowitz, M. *J. Phys. Chem. B* **1997**, *101*, 3793−3799.
(5) Conboy, J. C. *Investigation of Immisicible Liquid/Liquid Interfaces with Second Harmonic Generation and Sum-Frequency Vibrational Spectroscopy*; University of Oregon: 1996.
(6) Conboy, J. C.; Messmer, M. C.; Richmond, G. L. *J. Phys. Chem. B* **1997**, *101*, 6724−6733.
(7) Walker, R. A.; Conboy, J. C.; Richmond, G. L. *Langmuir* **1997**, *13*, 3070−3073.
(8) Dominguez, H.; Smondyrev, A. M.; Berkowitz, M. L. *J. Phys. Chem. B* **1999**, *103*, 9582−9588.
(9) Gragson, D. E.; Richmond, G. L. *J. Phys. Chem. B* **1998**, *102*, 569−576.
(10) Gragson, D. E.; Richmond, G. L. *J. Am. Chem. Soc.* **1998**, *120*, 366−375.
(11) Richmond, G. L. *Annu. Rev. Phys. Chem.* **2001**, *52*, 357−389.
(12) Shen, Y. R. *Nature* **1989**, *337*, 519.
(13) Bain, C. D. *J. Chem. Soc., Faraday Trans.* **1995**, *91*, 1281−1296.
(14) Miranda, P. B.; Shen, Y. R. *J. Phys. Chem.* **1999**, *103*, 3292−3307.
(15) Wei, X.; Miranda, B.; Shen, Y. R. *Phys. Rev. Lett.* **2001**, *86*, 1554−1557.
(16) Du, Q.; Freysz, E.; Shen, Y. R. *Science* **1994**, *264*, 826−8.
(17) Butcher, P. N.; Cotter, D. *The Elements of Nonlinear Optics*; Cambridge University Press: New York, 1990; Vol. 9.
(18) Boyd, R. W. *Nonlinear Optics*; Academic Press: New York, 1992.
(19) Shen, Y. R. *Surf. Sci.* **1994**, *299/300*, 551−562.
(20) Shen, Y. R. *The Principles of Nonlinear Optics*, first ed.; John Wiley & Sons: New York, 1984.
(21) Bloembergen, N. *Opt. Acta* **1966**, *13*, 311−322.
(22) Bloembergen, N.; Simmon, H. J.; Lee, C. H. *Phys. Rev.* **1969**, *181*, 1261−1271.
(23) Ong, S.; Zhao, X.; Eisenthal, K. B. *Chem. Phys. Lett.* **1992**, *191*, 327−335.
(24) Levine, B. F.; Bethea, C. G. *J. Chem. Phys.* **1975**, *63*, 2666−2682.
(25) Zhoa, X.; Ong, S.; Eisenthal, K. B. *Chem. Phys. Lett.* **1993**, *202*, 513−520.
(26) Levine, B. F.; Bethea, C. G. *J. Chem. Phys.* **1976**, *65*, 2429−2438.
(27) Bockris, J. O. M.; Reddy, A. K. N. *Modern Electrochemistry*, Second ed.; Plenum Press: New York, 1998; Vol. 1.
(28) Yeganeh, M. S.; Dougal, S. M.; Pink, H. S. *Phys. Rev. Lett.* **1999**, *83*, 1179−1182.
(29) Miranda, P. B.; Du, Q.; Shen, Y. R. *Chem. Phys. Lett.* **1998**, *286*, 1−8.
(30) Du, Q.; Freysz, E.; Shen, Y. R. *Phys. Rev. Lett.* **1994**, *72*, 238−41.
(31) Brown, M. G.; Raymond, E. A.; Allen, H. C.; Scatena, L. F.; Richmond, G. L. *J. Phys. Chem.* **2000**, *104*, 10220−10226.
(32) Wolfrum, K.; Laubereau, A. *Chem. Phys. Lett.* **1994**, *228*, 83−88.
(33) Scatena, L. S.; Richmond, G. L. *J. Phys. Chem. B* **2001**, *105*, 11240−11250.
(34) Conboy, J. C.; Messmer, M. C.; Richmond, G. L. *J. Phys. Chem.* **1996**, *100*, 7617−22.
(35) Bloembergen, N.; Pershan, P. S. *Phys. Rev.* **1962**, *128*, 606−622.
(36) Dick, B.; Gierulski, A. *Appl. Phys. B* **1985**, *38*, 107−116.
(37) Lobau, J.; Wolfrum, K. *J. Opt. Soc. Am. B* **1997**, *14*, 2505−2512.
(38) Scatena, L. F.; Brown, M. G.; Richmond, G. L. *Science* **2001**, *292*, 908−912.
(39) Scherer, J. R. The vibrational spectroscopy of water. In *Advances in Infrared and Raman Spectroscopy*; Clark, R. J. H., Hester, R. E., Eds.; Heyden: Philadelphia, 1978; Vol. 5; pp 149−216.
(40) Brown, M. G.; Richmond, G. L. (in preparation).
(41) Ataka, K.; Yotsuyanagi, T.; Osawa, M. *J. Phys. Chem.* **1996**, *100*, 10664−10672.
(42) Xia, X.; Perera, L.; Essmann, U.; Berk; Berkowitz, M. L. *Surf. Sci.* **1995**, *335*, 401−415.
(43) Eisenberg, D.; Kauzmann, W. *The Structure and Properties of Water*; Oxford University Press: New York, 1969.
(44) Birdi, K. S. *Self-Assembly Moonolayer Structures of Lipids and Macromolecules*; Kluwer Academic/Plenum Publishers: New York, 1999.
(45) Marcus, Y. *Ion Solvation*; Wiley: New York, 1986.
(46) Strauss, I. M.; Symons, M. C. R. *J. Chem. Soc., Faraday Trans* **1978**, *1*, 2518−29.
(47) Walrafen, G. E. *J. Chem. Phys.* **1971**, *55*, 768−792.
(48) Wall, T. T.; Hornig, D. F. *J. Chem. Phys.* **1967**, *47*, 784−92.

(49) Schultz, J. W.; Hornig, D. F. *J. Phys. Chem.* **1961**, *65*, 2131−2138.
(50) Walrafen, G. E. *J. Chem. Phys.* **1970**, *52*, 4176−98.
(51) Conrad, M. P.; Strauss, H. L. *J. Phys. Chem.* **1987**, *91*, 1668−1673.
(52) Danten, Y.; Tassaing, T.; Besnard, M. *J. Phys. Chem. A* **2000**, *104*, 9415−9427.
(53) Scatena, L. F.; Richmond, G. L. *Chem. Phys. Lett.* **2004**, *383*, 491−495.
(54) Israelachvili, J. N. *Intermolecular and Surface Forces*, Second ed.; Academic Press: London, 1992.
(55) Krichnerova, J.; Cave, G. C. B. *Can. J. Chem.* **1975**, *54*, 3909.
(56) Myers, D. *Surfaces, Interfaces, and Colloids*; VCH Publishers, Inc.: New York, 1991.